



OPEN

## Enhanced colon-targeted drug delivery through development of 5-fluorouracil-loaded cross-linked mastic gum nanoparticles

Umme Hani<sup>1</sup>, Nawaz Mahammed<sup>2✉</sup>, T Reshma<sup>3</sup>, Sirajunisa Talath<sup>4</sup>, Adil Farooq Wali<sup>4</sup>, Abdullah Aljasser<sup>5</sup>, Adel Al Fatease<sup>1</sup>, Ali H. Alamri<sup>1</sup> & Sharuk Khan<sup>6</sup>

This study explored the development of a novel colon-specific drug delivery system for 5-fluorouracil (5-FU) using cross-linked mastic gum (MG) nanoparticles (NPs). The primary goal is to enhance the treatment efficacy of colon cancer while minimizing systemic side effects. We employed Fourier Transform Infrared Radiation (FTIR) and Scanning Electron Microscopy (SEM) for the detailed characterization of the samples. FTIR analysis confirmed the successful cross-linking of MG, whereas SEM images revealed the spherical and uniform morphology of the NPs. Additionally, analysis of drug encapsulation efficiency (83.53%), particle size (240 nm), and drug release kinetics (zero-order), and the drug release percentage (95.20%) were analyzed. The results demonstrated that MG NPs effectively encapsulated and controlled the release of 5-FU in a colon-targeted manner. This study recommends the proposed drug delivery system because of its potential to improve the outcomes of colon cancer treatment.

**Keywords** Drug delivery, Polymer, Mastic gum, Sodium tri-metaphosphate, Nanoparticles, Colon cancer, 5-Fluorouracil

Oral colon-targeting systems are a significant development in the treatment of colon-related diseases, such as colon cancer, Crohn's disease, ulcerative colitis, and irritable bowel syndrome<sup>1</sup>. These systems delay medication release until they reach the targeted area in the cecum or colon, maximizing therapeutic efficacy and reducing side effects. Colon cancer, Crohn's disease, ulcerative colitis, and irritable bowel syndrome can be effectively treated with colon-targeted medication. Drugs that are destroyed in the upper gastrointestinal tract (GIT) are less likely to be absorbed systemically if they are delivered to the colon first<sup>2</sup>. The treatment of colonic diseases with regular medication administration devices is generally unsuccessful because of inadequate medication concentration at the site of action<sup>3</sup>. Therefore, it is difficult to find a treatment for these colonic illnesses that is both effective and safe for use in site-specific drug delivery<sup>4</sup>. To target the colon for drug delivery, harnessing the enzyme activity of the living bacteria is essential. The colon also has a longer retention period and responds well to treatments that increase the absorption of medications that are not very water-soluble. Owing to the makeup of bacteria in the colon, it is possible to create a drug delivery system tailored to that area. Colon-specific drug administration using degradable carriers has been studied, including guar gum, pectin, chitosan and dextrin<sup>5,6</sup>.

Cancer therapy, particularly for challenging types such as breast and colorectal cancer, has been significantly advanced by the development of innovative drug delivery systems (DDS). 5-Fluorouracil (5-FU), a cornerstone chemotherapeutic agent, is effective in treating various cancer types<sup>7</sup>. However, its clinical efficacy is hindered by its poor solubility, rapid systemic clearance, and high toxicity<sup>8</sup>. Nanoparticle-based DDS offer a transformative approach to address these limitations, enhancing therapeutic outcomes while minimizing side effects<sup>2,9,10</sup>. Recent research has focused on various nanoparticle systems for the delivery of 5-FU, including lipid-based, polymeric,

<sup>1</sup>Department of Pharmaceutics, College of Pharmacy, King Khalid University, Abha 62529, Saudi Arabia.

<sup>2</sup>Department of Pharmaceutics, Raghavendra Institute of Pharmaceutical Education and Research, K.R. Palli Cross, Anantapur, Chiyvedu 515721, Andhra Pradesh, India. <sup>3</sup>Department of Pharmaceutical Quality Assurance, Raghavendra Institute of Pharmaceutical Education and Research, K.R. Palli Cross, Anantapur, Chiyvedu 515721, Andhra Pradesh, India. <sup>4</sup>RAK College of Pharmacy, RAK Medical & Health Sciences University, Ras Al Khaimah, United Arab Emirates. <sup>5</sup>Department of Pharmaceutics, College of Pharmacy, Imam Abdulrahman Bin Faisal University, P.O. Box 1982, Dammam 31441, Saudi Arabia. <sup>6</sup>Department of Pharmaceutical Chemistry, N.B.S Institute of Pharmacy, Ausa, latur, Maharashtra, India. ✉email: mohammednawaz151@gmail.com

carbon-based, and inorganic nanoparticles (NPs), each presenting unique advantages, such as controlled drug release, targeted delivery, and improved bioavailability. The development of pH-responsive systems, particularly those based on polyacrylic acid (PAA), polyvinyl pyrrolidone (PVP), and carbon nanotubes (CNTs), is a significant advancement. These systems can effectively target the acidic tumor microenvironment, ensuring more precise and potent delivery of 5-FU<sup>11</sup>.

Novel methods of drug distribution that utilize natural polymers have been extensively studied over the past few decades. Natural polymers continue to be popular because of their low cost, abundance, biocompatibility, and degradability. MG is a natural biopolymer that can be used at low cost. The mastic tree (*Pistacia lentiscus*) in the family Anacardiaceae yields mastic resin. Human colorectal cancer cells have been proven to be susceptible to the antitumor action of MG extract in clinical testing. Therefore, MG was chosen as the vehicle for colon cancer therapy in this study. MG has been used in our previous studies to create diclofenac sodium sustained-release spheroids, and we examined the effect of roll compression on these pills<sup>12</sup>. However, there is no information in the literature regarding the preparation of phosphate-cross-linked MG NPs.

Within the scope of the current investigation, 5-FU was chosen as the model drug of choice (5-FU). Chemotherapy based on 5-FU is beneficial for patients with resection grade III colorectal cancer in terms of both overall and disease-free survival. Injecting 5-FU into a vein has harmful consequences throughout the body as its cytotoxic action spreads to abnormal areas. A less toxic and longer-lasting treatment can be achieved through colon-specific administration<sup>13</sup>. Chitosan NPs have been proposed to mitigate the harmful effects of 5-FU<sup>14</sup>. Therefore, attempts have been made to manage 5-FU's side effects by encasing the drug in biodegradable polymer NPs<sup>15,16</sup>.

The integration of natural polymers and nanoparticle-based DDS in colon-targeted systems represents a major advancement in the treatment of colorectal cancer and other colon-related diseases. This combination offers benefits, such as targeted delivery, reduced systemic effects, enhanced drug efficacy, and more effective and less toxic treatment options for patients.

The novelty of this study lies in the formulation and evaluation of cross-linked MG NPs for colon-targeted drug delivery of 5-FU. This approach is distinct in its use of natural gum as a biodegradable and biocompatible material for drug encapsulation and controlled drug release. Additionally, the specific cross-linking technique employed enhanced the stability and targeted delivery capabilities of the NPs<sup>17,18</sup>.

## Mechanisms of nano-drug delivery

### Targeted delivery

NDDS are engineered to selectively deliver drugs to specific cells or tissues such as cancer cells or inflamed tissues. This targeting is achieved through the surface modification of NPs with specific ligands or antibodies. These molecules are chosen for their ability to bind to receptors or antigens that are overexpressed or uniquely present in target cells.

For example, in cancer therapy, NPs can be functionalized with antibodies that recognize and bind to tumor-specific markers. This results in a higher concentration of the drug at the tumor site, maximizing its therapeutic effect, while minimizing damage to healthy cells<sup>19</sup>.

### Controlled release

Controlled release refers to the ability of nanocarriers to release an encapsulated drug at a predetermined rate over a specific period. This is achieved by designing the matrix of the NPs to respond to certain physiological triggers, such as changes in pH, temperature, or the presence of specific enzymes. For instance, NPs can be designed to remain stable in the bloodstream, but release their payload when they reach the acidic environment of a tumor or inflamed tissue. This controlled release helps maintain the therapeutic level of the drug over an extended period, reducing the need for frequent dosing<sup>20,21</sup>.

### Enhanced permeability and retention (EPR) effect

The EPR effect is a phenomenon primarily observed in solid tumors. Tumors have unique vasculature that is often poorly organized and leaky, coupled with a deficient lymphatic drainage system. These characteristics allow NPs to passively accumulate in tumor tissues. NPs, owing to their small size, can exploit these abnormalities to preferentially accumulate in tumor sites. This passive targeting mechanism is one of the primary reasons NDDS is particularly promising for cancer therapy<sup>22</sup>.

### Improved solubility

Many drugs have poor water solubility, limiting their bioavailability and therapeutic efficacy. NPs can enhance the solubility of these drugs by encapsulating them within a soluble matrix or altering their physical state. By improving solubility, NPs help in better absorption of the drug in the gastrointestinal tract after oral administration or in circulation after parenteral administration. This leads to better drug distribution in the body and enhanced therapeutic effectiveness<sup>23</sup>.

### Need of nanoparticle-based delivery

NPs have emerged as pivotal tools in targeted drug delivery for colon cancer treatment, leveraging their unique physicochemical properties to address the critical challenges of specificity, reduced systemic toxicity, and drug resistance. Exploiting the EPR effect, NPs preferentially accumulate at tumor sites, minimizing exposure to healthy tissues. This selective accumulation is further augmented by modifying nanoparticle surfaces with ligands or antibodies targeting specific molecular markers in colon cancer cells, thereby enhancing the uptake of therapeutic agents<sup>24</sup>. Encapsulation of drugs within NPs protects them from premature degradation and

enables controlled release at the tumor site, maintaining therapeutic levels for prolonged periods. This approach significantly mitigates systemic toxicity and counteracts drug resistance, which are common hurdles in effective colon cancer chemotherapy<sup>25</sup>. Moreover, NPs facilitate combination therapy by carrying multiple drugs, offering a synergistic approach to overcome resistance through multimodal mechanisms.

The application of NPs in colon cancer treatment exemplifies a strategic advancement in oncology, promising enhanced chemotherapy efficacy, while minimizing adverse effects. Their capacity for targeted delivery, combined with the potential for surface modification and controlled release, underscores the transformative potential of nanoparticle-based DDS in improving therapeutic outcomes in colon cancer patients<sup>26</sup>.

### Toxicity report

A toxicity report on MG revealed that after 13 weeks of dietary administration to F344 rats at varying doses (0%, 0.22%, 0.67%, and 2%), no mortality or clinical signs were observed. High doses resulted in decreased body weights (especially in males) and increased liver weights in a dose-dependent manner, without morphological changes in the organs examined. Other changes included alterations in hematological and serum biochemical parameters. The study concluded that MG has a no observed adverse effect level (NOAEL) of 0.67% in the diet<sup>27</sup>.

### Study on MG

MG demonstrates multifaceted pharmaceutical potential across various applications, from enhancing drug bioavailability to serving as a therapeutic agent with broad biological activity. A study utilizing Amoxicillin Trihydrate (ATH) microspheres combined with MG showed an improved *in vivo* drug level and faster systemic circulation, suggesting MG's capability to enhance ATH's bioavailability of ATH in healthy rabbits<sup>28</sup>. This study provides an extensive review of MG's biological activities of MG, including its antimicrobial, anti-inflammatory, antioxidant, and anticancer properties, highlighting its significance in both traditional and modern medicinal applications<sup>29</sup>. This study explored MG's application of MG in drug delivery systems, particularly as a compression coat for the colonic delivery of 5-FU, indicating its potential to improve the efficacy and targeting of cancer treatment drugs. Collectively, these studies underscore the valuable contributions of MG to pharmaceutical research and its potential in medical treatments<sup>30</sup>.

### Materials and methods

The pure drug 5-FU was procured from Hi-media, Mumbai. MG was purchased from the Chios Gums Mastic Farmers Association, Chios, Greece; where it is grown, and it was of commercial quality. Sodium trimethyl phosphate (STMP) was obtained from Sigma Aldrich, Mumbai, India. All other chemicals, reagents, and solvents used were of high quality and High-performance liquid chromatography (HPLC) grade.

### Preparation of phosphate cross-linked mastic gum nanoparticles (MGNPs)

The cross-linked MGNPs were prepared in two steps: the aqueous phase was prepared first, followed by the organic phase. The aqueous phase was then gradually added to the organic phase and homogenized<sup>31–33</sup>. Below is a detailed breakdown of the steps undertaken to obtain NPs, which are also illustrated in Fig. 1. The Fig. 1 is prepared by using Inkscape 1.0.2 (<https://inkscape.org/release/inkscape-1.0/?latest=1>).

#### Aqueous phase

To prepare the MG solution, as much as 4% (w/v) of MG was dissolved in 10 ml of a 2 M sodium hydroxide (NaOH) solution in a beaker. STMP solution (1–4% w/v) was prepared by mixing 10 ml of distilled water with STMP in a beaker. The solution of MG that was distributed and the STMP aqueous phase for 5-minute solution were combined using homogenization.

#### Organic phase

At 50 °C, 150 ml of liquid paraffin (16 mm<sup>2</sup>/sec at 50 °C) was added to a beaker with 3% weight-per-volume (w/v) Span 80 while being agitated. This occurred during the organic stage. To create an emulsion-free version, the aqueous phase was slowly added to the beaker while spinning at a high speed (6000 rpm). At 50 °C and 6000 rpm, a cross-linking reaction occurred. After 8 h of cross-linking, the particles were separated by centrifugation at 15,000 rpm for 30 min and washed three times in acetone. After 12 h of drying at 40 °C, the cross-linked MG NPs were stored in airtight containers for further research. Table 1 provides the formulas for the synthesized cross-linked MG NPs.

### Measurement of particle size and zeta potential

Using a Malvern Zetasizer Nano-ZS90 equipped with a photon correlation spectrometer (PCS), we determined the MG nanoparticle size and zeta potential (Malvern Instruments, UK). The degree of particle size distribution was analyzed at room temperature and a dispersion angle of 90°. The particle dispersion was filtered through a 0.22 mm membrane after being appropriately diluted with pure water (1 ml in 25 ml). The diameter was calculated as the mean ± SD of three separate parallel measurements (standard deviation).

### Scanning electron microscopic (SEM)

At room temperature, SEM images were captured at the necessary magnification using a SEM of the USA-made Joel-LV-5600 model. Overnight, the NPs were evaporated in vacuum after being placed on a metal stub with a glass disc glued to it. Argon plasma sputtering was used to deposit a gold palladium coating 10 nm thick onto the samples and environment before SEM analysis (EMITECH-K550 Sputter Coater, Houston, TX, USA).

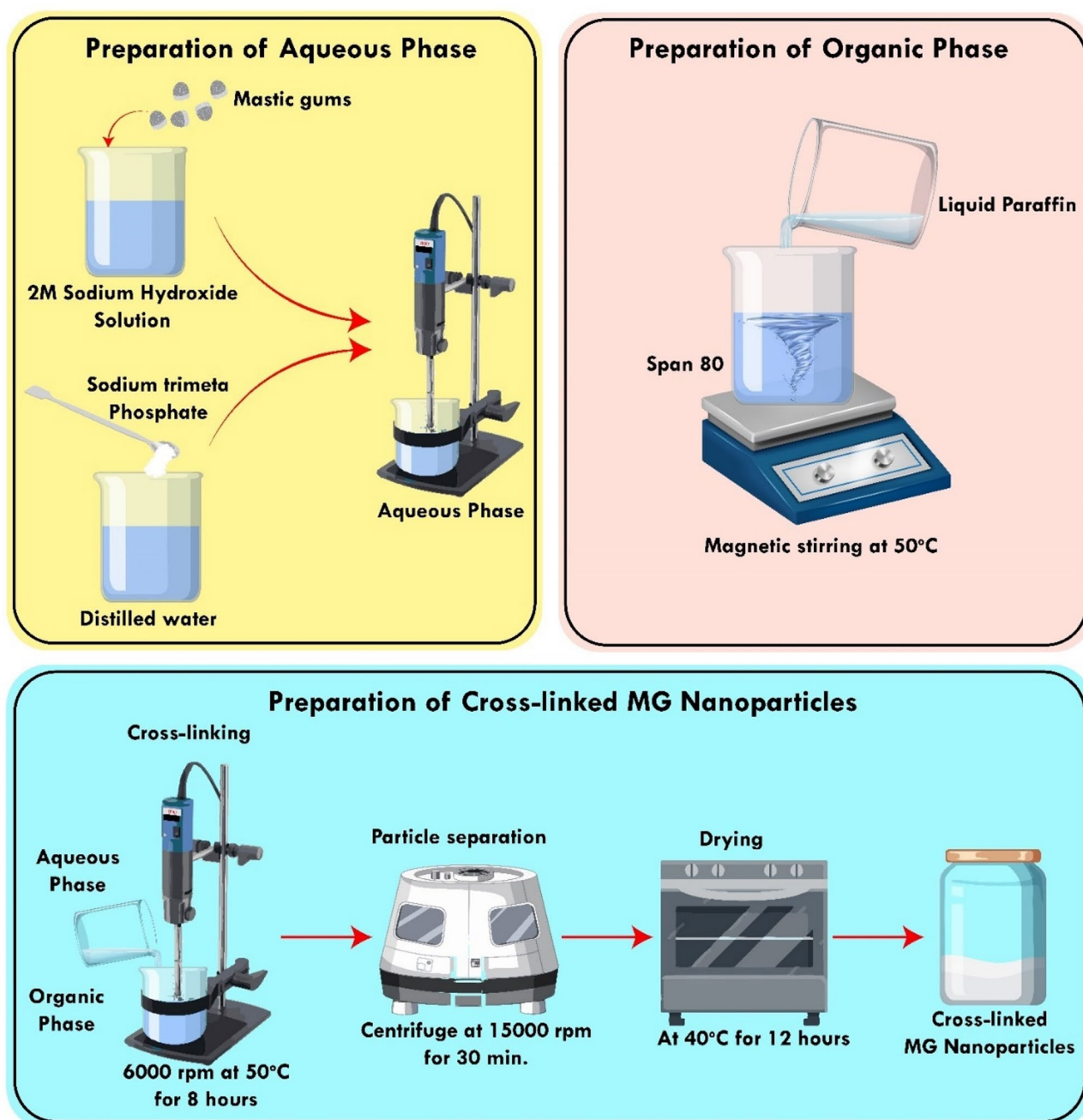


**Fig. 1.** Detailed illustration of preparation of phosphate crosslinked MGNPs. [Inkscape 1.0.2 (<https://inkscape.org/release/inkscape-1.0/?latest=1>)].

#### Differential scanning calorimetry (DSC)

The 2010 DSC module of the Thermo analyzer made by Du Pont was used for DSC research (USA). Extremely high-purity indium metal was used to calibrate the instrument. Nitrogen gas was used as the environment and a heating rate of 10 °C/min was used for the dynamic scans.

#### Fourier transform infrared radiation measurements (FTIR)

The KBr pellet method on a Shimadzu FTIR spectrophotometer (model 8033, USA) was used to conduct FTIR analysis of MG, cross-linked MG, pure drug, and nanoparticle-containing drug.

#### Swelling studies

The conventional gravimetric technique was used to investigate the swelling of native MG and cross-linked MG NPs, as reported previously<sup>34</sup>. NPs (100 mg) were measured after swelling in a known volume (10 mL) of Tris buffer (pH 6.8) contained within a sintering glass furnace (pore size, 5–10 m). for a predetermined period of

Formulation code	5-FU(mg)	Mastic Gum (mg)	STMP(mg)	Liquid paraffin(ml)
MG1	50	100	100	150
MG2	50	100	200	150
MG3	50	100	300	150
MG4	50	200	100	150
MG5	50	200	300	150
MG6	50	300	100	150
MG7	50	300	200	150
MG8	50	400	100	150
MG9	50	400	300	150

**Table 1.** Formulation chart of prepared cross-linked MG NPs.

time. Nanoparticle swelling was continually monitored with no additional increase in nanoparticle weight after 15 min, indicating the onset of optimum swelling conditions. The following equation was used to determine nanoparticle water uptake:

$$\text{Swelling ratio} = W_t/W_o \quad (1)$$

where the dry nanoparticle weight,  $W_o$ , and swollen nanoparticle weight,  $W_t$ , are measured at time zero and time  $t$ , respectively.

### Drug loading and encapsulation efficiency

Ten mg of phosphate buffer (pH 7.4), and the NPs were disseminated throughout the buffer. The sample was ultrasonically treated for 10 min, split across three separate sessions. After filtering the solution, 1 ml was poured into a 10 ml volumetric flask to the appropriate concentration. Using a UV absorption spectrophotometer, the absorbance was determined at 267 nm<sup>35</sup>. The drug concentration was determined using the following equation:

$$\text{Amount of Drug} = \text{Concentration} \times \text{Dilution Factor}$$

The following formulae were used to determine the drug-loading percentage and encapsulation efficiency:

$$\% \text{ Drug Loading} = \text{Weight of Drug in Nanoparticles} \times 100$$

$$\text{Encapsulation Efficacy} = \text{Actual Drug Content} \div \text{Theoretical Drug Content} \times 100$$

### In vitro drug release studies

Research into the rate and extent to which 5-FU was released from cross-linked MG NPs was conducted using a dissolution test conducted using the pH progression method in accordance with the U.S. pharmacopoeia (Basket type, 100 rpm, 37.0 °C) in simulated gastric fluid (SGF) of pH 1.2 for 2 h, simulated intestinal fluid (SIF) of pH 4.5 for 3 h, and SIF of pH 7.4 for following 3 h. At regular intervals, 1 ml of the sample was taken, and to maintain the sink's condition, the old medium was replaced with a similar volume of fresh medium. The tissue samples were withdrawn and tested for drug release using a UV absorption spectrophotometer at 267 nm<sup>35</sup>.

### In vivo studies

The in-vivo procedure was performed according to the guidelines of the Committee for Control and Supervision of Experiments on Animals (CCSEA)<sup>36</sup>. The Institutional Animal Ethical Committee at Raghavendra Institute of Pharmaceutical Education and Research-Autonomous in Andhra Pradesh approved this project (code: 878/PO/Re/S/05/CPCSEA). For the in-vivo experiment, Twelve healthy albino rats were selected for in vivo experiments. The albino rats used in this study were sourced from Vyas Laboratories 22,125, Amberpet, Hyderabad – 500,013, India. Formulation MG5 was chosen based on in vitro drug release. The albino rats used in the in-vivo studies were all of similar size, and the rats were fed a normal rodent diet but fasted for 24 h before the study. A total of 12 animals were divided into three groups of 4. One group served as a control, another received a 5-FU solution (dosage determined by the animal's body weight), and a third received cross-linked MG NPs after preparation (MG5). The medicines were administered through a cannula. We isolated the stomach, small intestine, and a portion of the large intestine from a third group of mice that were sacrificed at 2, 4, 6, and 8 h to estimate the percentage of medication absorbed up to 8 h from the standard group. These organs were homogenized in phosphate-buffered saline (PBS; pH 7.4) in a modest volume, and then 1 ml of acetonitrile was added. HPLC was used to determine the concentration of the separated supernatant after centrifugation.

The rat was gently restrained to minimize stress and was placed on a stable surface with the abdomen exposed. The lower right quadrant of the abdomen was used as the injection site. The needle was inserted at a shallow angle (10°–15°) into the peritoneal cavity, and a dose of 800 mg/kg was administered. Aspiration was performed gently to ensure that the needle had not entered the blood vessels or bladder. The calculated dose of sodium pentobarbital was slowly injected.

The animal was placed back into its cage and monitored for signs of anesthesia onset, such as loss of righting reflex and decreased respiratory rate. Death was confirmed by the absence of vital signs. As a secondary measure, a physical method, such as cervical dislocation or bilateral thoracotomy, was performed to ensure euthanasia<sup>37</sup>. All in-vivo work is in vivo studies complied with the ARRIVE criteria. This study was conducted in accordance with ARRIVE guidelines<sup>38</sup>.

### Preparation of rat enzymes induced cecal medium

To prepare rat enzyme-containing cecal medium, we repurposed a previously described procedure (Jain et al., 2007). To maintain their weight, normal diet-fed rats weighing approximately 150 to 200 g received an intraperitoneal injection of 1 ml of 1% w/v solution of Ms in saline. Seven days later, this therapy was administered. The rats' cecums were removed and ligated at both ends after they were humanely killed. After being untied, the cecum was transported to the SIF (pH 7.4) where carbon dioxide bubbles were added to keep the environment anaerobic. An incubation period of 24 h was applied to the solution to guarantee adequate bacterial multiplication and enzyme production. Following this, the suspension was filtered using Whatman filter paper no. 42 and resuspended in buffer to reach the desired concentration of 4% w/v. Dissolution experiments used this solution to mimic intestinal fluid. Different drug release models, including the zero-order, first-order, Higuchi, Hixon-Crowell cube root law, and Korsmeyer-Peppas models, were used to investigate the drug release mechanism from in-vitro studies.

### Chromatographic conditions

The quantitative detection of 5-FU in the plasma and the drug it contains was achieved using HPLC. created It is sensitive, reproducible, selective, and accurate. Isocratic elution was used to achieve separation using a genesis C18 column and a pH 3.2 (perchloric acid) solvent combination of methanol and water (10:90v/v), flowing at a rate of 1.0 ml/min. room temperature. Dimensional analysis of the concentration peaks and mg per ml were used to quantify the results. 5-FU has a retention time of 4.5 min<sup>39</sup>.

### Stability studies

In accordance with the ICH Quality Guidelines (2003), a stability study of the optimized nanoparticle formulation was conducted to evaluate its physicochemical stability under different storage conditions. The NPs were stored for 90 d under real-time (25 °C/55–60% RH) and accelerated (40 °C/75% RH) conditions to simulate both normal and extreme environmental conditions. Samples were withdrawn at predetermined intervals of 15, 45, and 90 days and analyzed for visual changes, drug content, and zeta potential to assess any possible degradation, aggregation, or physicochemical instability. The selection of these conditions ensures a comprehensive understanding of the shelf-life, stability, and potential for long-term storage of the formulation, which is crucial for its further development and clinical applications.

## Results and discussion

The emulsion cross-linking approach was successfully used to create cross-linked MG NPs. To create an aqueous phase, the organic phase was emulsified without an emulsion. in the presence of an emulsifier. The temperature, specifically 50 °C, triggered a crosslinking event, and an emulsification process encased the drug particles. Additionally, the homogenization velocity was used in the formation of the NPs. The pH of the cross-linked MG was 5.8 0.59. This is helpful for the development of medicinal dosage forms because it does not irritate the mucous membrane and epithelium<sup>40</sup>.

### Particle size and zeta potential analysis

NPs enable efficient drug accumulation at the target site because of their small size, allowing them to pass through narrow capillaries and be taken up by cells<sup>41</sup>. In this study, the produced NPs had an average size range of 121.5 ± 2.28 nm to 391.5 ± 1.28 nm, as presented in Table 2. The particle size increased proportionally with the polymer content in different formulations (MG1 to MG9). This increase was attributed to the increase in viscosity at higher polymer concentrations, leading to the formation of larger droplets during emulsification. Additionally, increasing the homogenization speed beyond 8,000 rpm did not yield smaller particles, likely

Formulation code	Average particle size	Zeta potential (mV)	Entrapment efficiency (%)	Drug loading (%)
MG1	321.5 ± 2.28	-19.9 ± 1.9	74.46 ± 1.22	24.17 ± 0.40
MG2	342.11 ± 0.98	-22.3 ± 0.78	65.96 ± 0.34	21.8 ± 0.12
MG3	376.98 ± 1.98	-22.92 ± 1.54	53.78 ± 0.68	17.75 ± 0.22
MG4	398.25 ± 2.33	-23.45 ± 2.58	73.51 ± 1.61	14.7 ± 0.322
MG5	425.23 ± 1.88	-26.8 ± 2.1	83.53 ± 1.21	16.7 ± 0.24
MG6	480.25 ± 2.66	-21.92 ± 0.54	48.78 ± 0.81	6.83 ± 0.11
MG7	531.47 ± 2.34	-20.98 ± 2.75	82.66 ± 1.58	11.57 ± 0.22
MG8	563.85 ± 1.84	-21.98 ± 0.75	52.78 ± 1.16	5.80 ± 0.12
MG9	591.5 ± 1.28	-20.11 ± 0.89	61.59 ± 1.41	6.79 ± 0.15

**Table 2.** Average size, zeta potential, entrapment efficacy and drug loading values of all formulations.

because of emulsion destabilization at excessive shear forces. Conversely, lower homogenization speeds result in larger droplets coalescing into bigger particles<sup>42</sup>. The stability and adsorption qualities of biomolecules are largely determined by the nature and amplitude of the zeta potential of NPs. Particles aggregate and precipitate if the zeta potential is below a certain threshold value. To ensure uniform polymer distribution in the oil phase, Span-80 was used as an emulsifier. The required emulsifier concentration was critical; at insufficient levels, the interfacial tension was not adequately reduced, leading to droplet coalescence and the formation of larger globules. The zeta potential of the NPs ranged from  $-19.9 \pm 1.9$  mV to  $-26.8 \pm 2.1$  mV, influencing their stability. A zeta potential of  $-26.8 \pm 2.1$  mV (observed in MG5) was optimal for maintaining nanoparticle stability by preventing aggregation through electrostatic repulsion. The presence of cross-linked STMP polymers, which contain phosphate groups, contributes to the negative surface charge of the NPs<sup>43</sup>.

### SEM studies

The shapes and morphologies of the nanoparticle surfaces were studied using SEM. Photographs taken with a scanning electron microscope are shown in Fig. 2 (A) and (B). The drug-loaded NPs in the MG5 formulation were well-defined, spherical, and had a smooth surface (B). The medicine is likely evenly distributed throughout the nanoparticle carrier if no crystalline formations can be observed on their surface. The medication is molecularly diffused equally throughout the polymer matrix, and, to the best of our knowledge, all particles are round and have a rough exterior.

### DSC and FTIR studies

DSC and FTIR spectroscopy analyses substantiate the absence of interaction between the polymer and 5-FU, as demonstrated by consistent melting points (at 280 °C and 278.89 °C) in the DSC thermograms (Fig. 3). The IR spectrum revealed the characteristic O-H (at 32503600  $\text{cm}^{-1}$ ) broad peak of MG and its alteration after cross-linking with STMP, indicating the formation of phosphor diester bonds and successful cross-linking. This alteration in the IR spectrum, along with the retained alkane C-H stretching (at 2850  $\text{cm}^{-1}$ ) and methane glycol methane peaks (at 1375  $\text{cm}^{-1}$ ), confirms MG's structural integrity post-cross-linking.

### Swelling studies

Water and digestive fluids cause native MG to expand by a factor of 80–100. (Deshpande et al., 2013). The total edema of the MG was reduced owing to cross-linking with STMP (Fig. 4a). This is because water molecules that create hydrogen bonds with the hydroxyl group of MG are blocked by the cross-links created by the swelling of cross-linked MG.

### Drug loading and encapsulation efficiency

This study explored the effect of MG concentration on the encapsulation efficiency (EE) and drug loading (DL) of NPs, revealing that EE values fluctuated between 48.78% and 83.53% across different formulations. Formulations with higher MG concentrations, specifically MG5 and MG7, demonstrated the highest EE. This correlation underscores the direct influence of the amount of MG on EE. Similarly, DL was positively affected by MG concentration, indicating that higher MG levels enhanced drug loading capacities.

The inherent properties of MG, including viscosity, molecular weight, and matrix-forming ability, are crucial in achieving effective encapsulation and drug loading. The viscosity of the solution, dictated by the MG concentration, influenced the emulsion droplet size during nanoparticle preparation, with smaller droplets fostering increased EE and DL owing to their larger surface area for drug interaction. Furthermore, the cross-

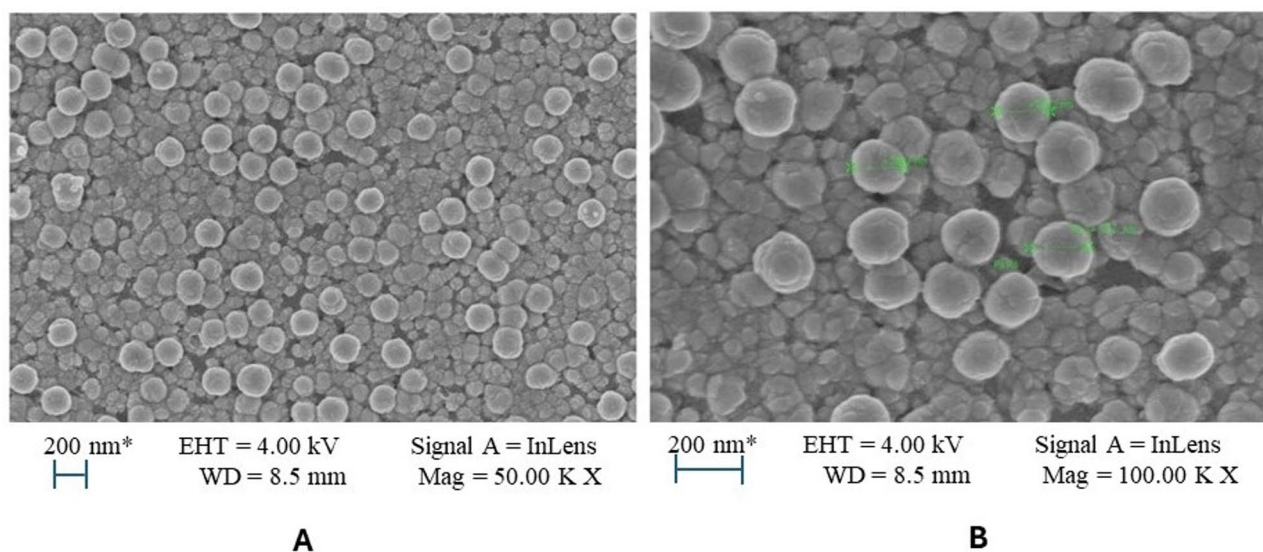


**Fig. 2.** (A) & 1(B): SEM images of the optimized formulation.

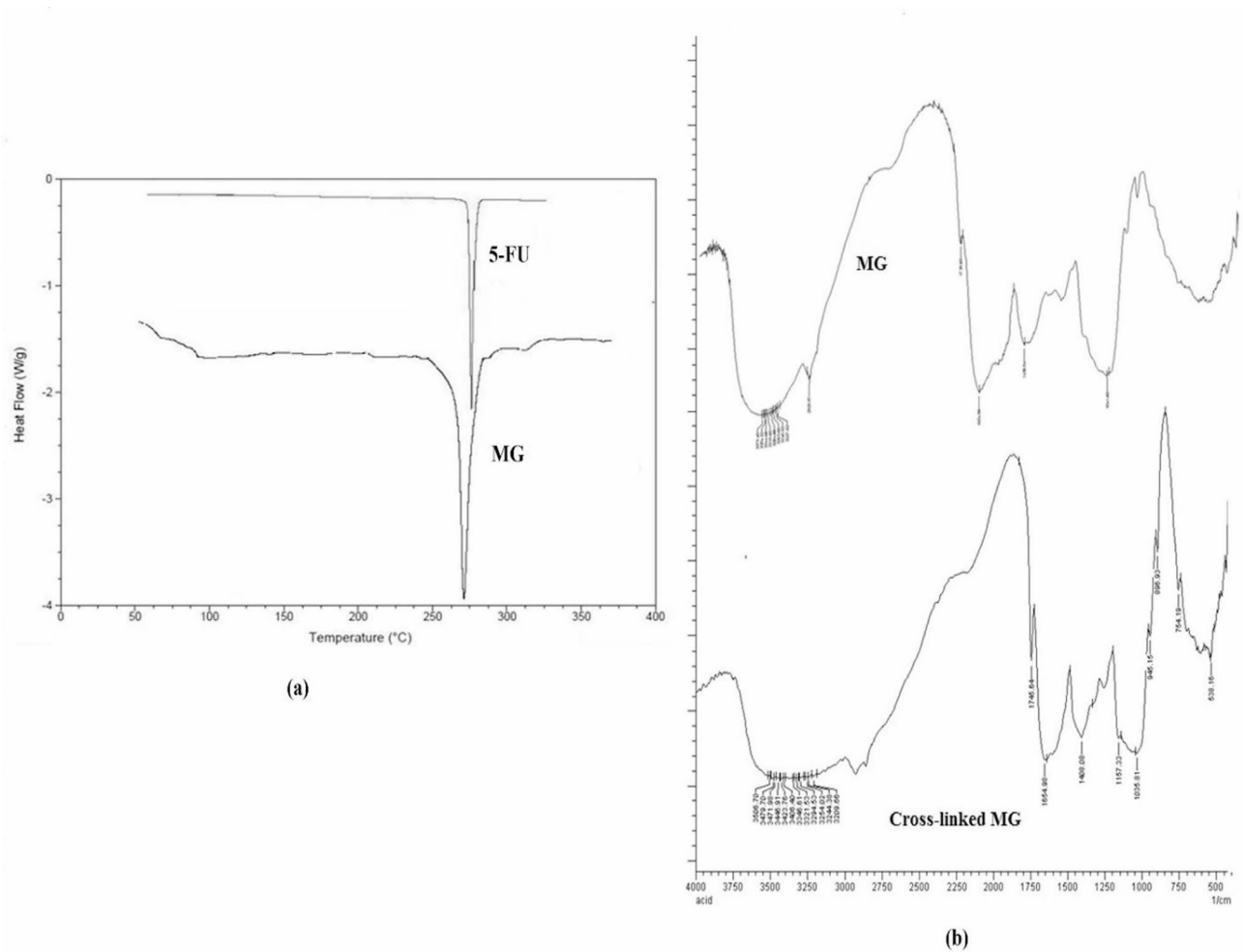


**Fig. 3.** (a) Overlay DSC thermogram of the drug and MG, and (b) overlay FTIR spectra of MG and cross-linked MG.

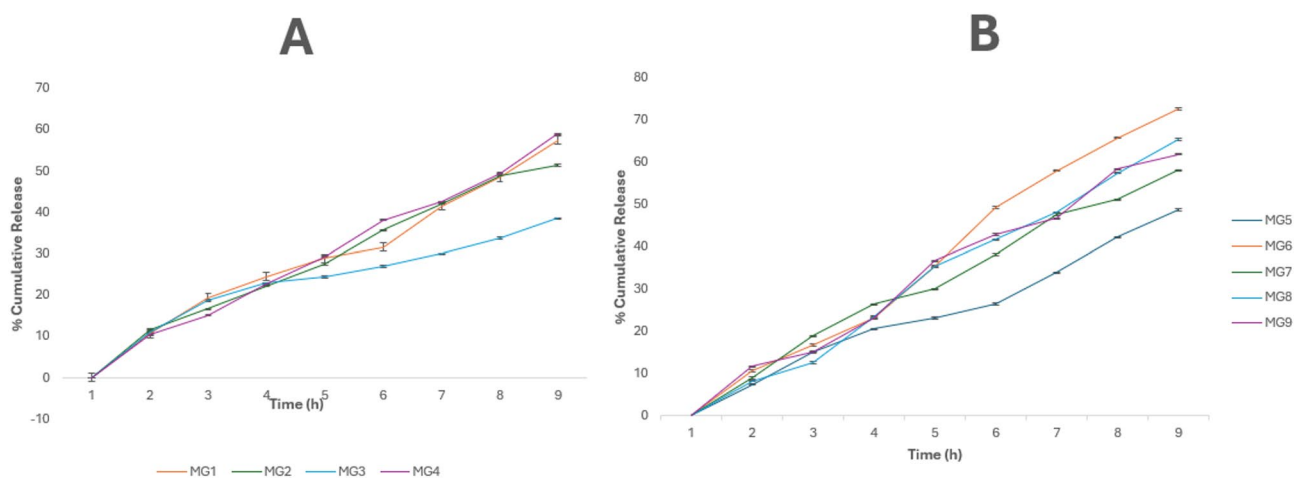


**Fig. 4.** (a) In vitro release profiles for formulations from MG1 to MG4 and (b) In-vitro release profile for formulations from MG5 to MG9.

linking of MG with STMP affected the structural and porosity characteristics of the NPs, impacting the EE and DL outcomes. MG's concentration of MG and its cross-linking behaviour significantly determine the EE and DL of the nanoparticle formulation, highlighting the necessity of optimizing these parameters to enhance the efficacy of the drug delivery system.

#### *In vitro drug release studies*

Drug release profiles for various nanoparticle formulations (MG1–MG9), showing the percentage of drug release over time (up to 8 h). In-vitro release data for 5-FU NPs from MG1 to MG9 are shown in Fig. 4. All synthesized nanoparticle formulations exhibited enhanced drug release in SIF at pH 7.4, starting at the sixth hour. The percentage of crosslinking agents used influenced the drug release profile. Depending on the ratio of gum to the cross-linking agent, the drug was released at different rates after the NPs were gradually degraded by pancreatic and bacterial colonic enzymes. In a SIF release study, MG5 showed a drug release rate of 82.61% when MG and STMP were mixed in a 2:3 ratios. Through MG-STMP cross-linking, the proportion and excessive expansion of MG can be prevented, thus avoiding a delay in drug release by blocking the access of water to its hydroxyl group. In the conclusion of the eighth, the medication was released at a rate of 72.41% in MG2 and MG7 containing a 1:2 ratio of MG and STMP, respectively. Since MG is cross-linked with a large amount of STMP, the drug release from MG3 containing a 1:3 ratio of MG and STMP was 38.17%. There was a Drug release was 52.72% and 55.33%, respectively, from MG6 and MG8, which included MG and STMP in ratios of 3:1 and 4:1, respectively. If an adequate failure to cross-link all of the MG molecules using STMP results in significant swelling of the gum and slows the release of the medication, the drug release in these formulations is very high in the sixth, then the 7th and 8th saw almost no relief. The MG5 formulation performed well in terms of % CDR after 8 h in SIF at pH 7.4. As can be seen in Fig. 4, MG5 was dissolved in a media using 4% (enzyme-induced) rat cecal material for 3 h to see how release is affected changes when these enzymes are present (b). pH 1.2 and pH 4.5 SGF and SIF only released 27.3719% of the medication. Due to in the enzymes induced rat anal sac media, the proportion of polysaccharide digested by enzymes produced by colonic micro flora medication found in the medium of rat cecal content 43.8114% after 6 h, and release was further enhanced to 95.2018% at 8 h<sup>44</sup>. A statistical method called analysis of variance (ANOVA) was used to examine the results (ANOVA). Differences were considered significant at the level of significance ( $p < 0.05$ ).

#### *In vivo studies*

The data showed that after taking 5-FU in the form of a basic medication suspension (standard), the cancerous cells were killed. Two hours after administration, 9.74% of 5-FU was absorbed, and by hour eight, 41.33% had been absorbed. Absorption rates of 17.74% were recorded in the upper GIT, indicating that the cross-linked NPs of formulation (MG5) were generally intact there (0–5 h). On day 8, the body absorbed 63.52% of the medication. Table 3 displays the HPLC data obtained from the in vivo experiments.

HPLC findings indicated that the nanoparticle formulation (MG5) showed a distinct absorption profile in the gastrointestinal tract compared to the standard formulation, suggesting that the NPs provided a more targeted and controlled release of the drug in the colon. The HPLC data and its interpretation provided evidence for the efficacy of the MG nanoparticle system in achieving colon-targeted drug delivery.

#### *In vitro and in vivo correlation studies (IVIVC)*

In vitro to in vivo correlation (IVIVC) represents a pivotal concept in pharmaceutical research and development, facilitating the streamlining of the drug development cycle and enhancement of drug formulations (Fig. 5). By establishing a reliable correlation between in vitro (laboratory-based) studies and in vivo (animal- or human-based) outcomes, IVIVC enables the prediction of a drug's behavior within a biological system based on its performance in controlled laboratory settings. This predictive capability is instrumental in optimizing dosage forms, reducing reliance on extensive human trials, and potentially substituting certain bioequivalence studies, provided that dissolution acceptance criteria are met. Regulatory bodies, such as the International Council for Harmonization (ICH), endorse IVIVC for its role in improving drug development efficiency and safety<sup>45,46</sup>.

A profound IVIVC is characterized by a strong positive relationship between the amount of drug released in vitro and the extent of its absorption in vivo, as indicated by high regression coefficients (e.g.,  $R^2=0.96$ ). Such correlations are essential for validating the use of in vitro drug release profiles as reliable predictors of in vivo drug performance. The selection of appropriate mathematical models, such as the zero-order kinetics model, which suggests a constant drug release rate independent of concentration, further supports the accurate prediction of in vivo drug behavior from in vitro data.

Time (h)	Standard			Formulation MG5			
	Peak Area	Plasma drug concentration (µg/ml)	% drug absorbed	Peak Area	Cecal drug concentration (µg/ml)	Plasma drug concentration (µg/ml)	% drug absorbed
2 h	346,036	6.89	9.74	995,922	19.83	4.17	5.66
4 h	288,782	5.75	22.46	856,302	17.05	6.95	17.77
6 h	237,554	4.73	32.97	772,436	15.38	8.62	33.93
8 h	184,820	3.68	41.33	606,693	13.68	10.32	53.52

**Table 3.** HPLC data of standard and formulation MG5.

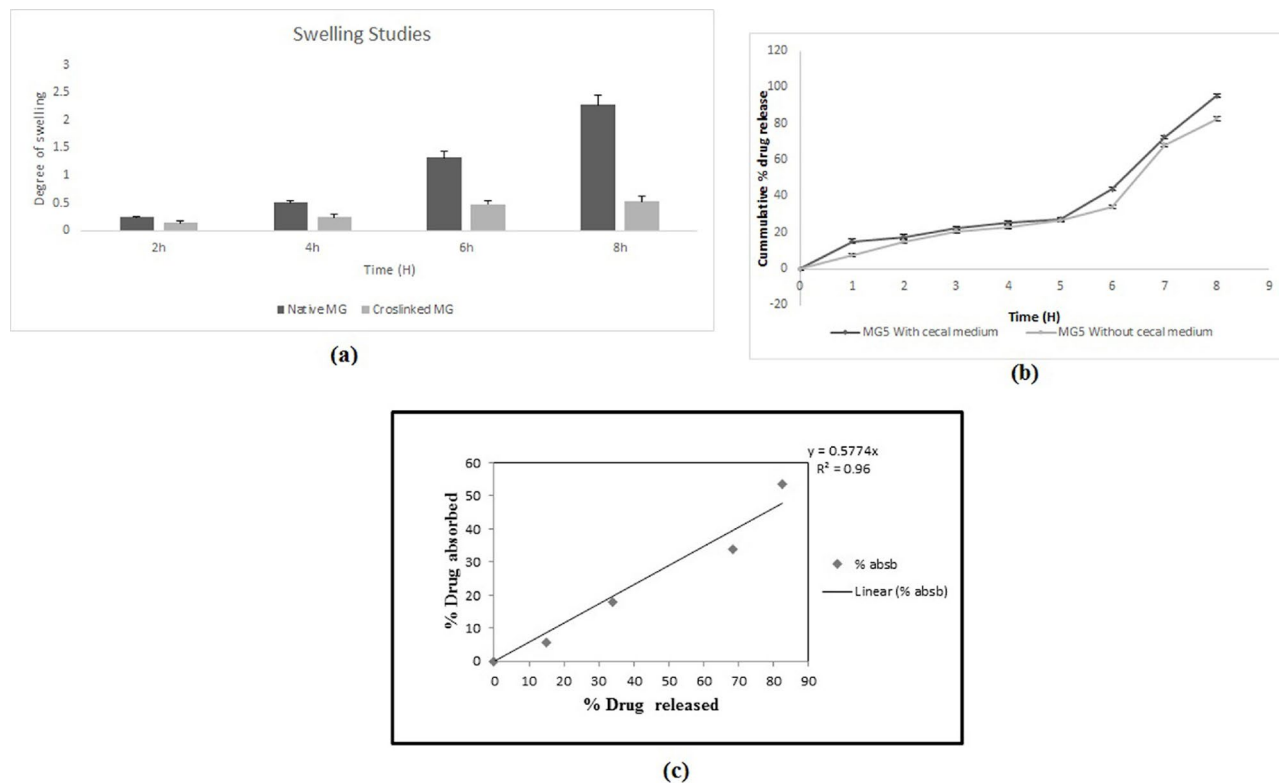


**Fig. 5.** (a) Swelling studies, (b) Percentage drug release studies and (c) *In vitro-In vivo* correlation.

The integration of *IVIVC* into pharmaceutical R&D not only enhances the predictability of drug-release mechanisms but also aligns with regulatory expectations for evidence-based drug development practices. This synergy between predictive modelling and empirical evidence offers a robust framework for advancing pharmaceutical innovations, while ensuring patient safety and therapeutic efficacy.

### Stability studies

Periodic evaluations of the samples for visual changes, drug content, and zeta potential revealed the sustained chemical and physical stability of the nanoparticle formulation throughout the stability study. No significant alterations in drug content or zeta potential were observed, indicating no drug interactions or degradation within the formulation. The maintained zeta potential suggested effective particle dispersion and aggregation prevention. These results validated the robustness of the MG nanoparticle formulation for drug delivery, highlighting its suitability for long-term storage and its potential to preserve therapeutic efficacy and safety for clinical use.

### FDA approval

MG is a natural resin obtained from the *Pistacia lentiscus* tree that has been traditionally used for various purposes, including its potential health benefits. However, it is important to note that dietary supplements, including mastic gum, are not regulated by the U.S. Food and Drug Administration (FDA) in the same manner as pharmaceutical drugs. Dietary supplements, including MG products, do not undergo the same rigorous testing and approval processes as prescription drugs. Instead, the FDA regulates dietary supplements under the Dietary Supplement Health and Education Act (DSHEA). Manufacturers are responsible for ensuring the safety and labelling of their products, but are not required to obtain FDA approval before marketing them.

The formulation, designated MG5, showed promising results in terms of drug release, encapsulation efficiency, and targeted delivery to the colon, minimizing systemic absorption and potential side effects. This study presents a comprehensive and scientific approach that is favorable for FDA approval in clinical studies.

### Conclusion

This study successfully developed a novel colon-specific drug delivery system using cross-linked MG NPs for 5-FU encapsulation with the aim of enhancing treatment efficacy while minimizing systemic side effects. The use of MG as a biodegradable, biocompatible carrier, and the specific cross-linking technique employed contributed to the stability of the formulation and targeted release properties. Characterization through FTIR and SEM confirmed successful cross-linking and uniform nanoparticle morphology, with significant encapsulation efficiency (83.53%) and controlled drug release kinetics (zero-order). The optimized formulation (MG5) demonstrated a particle size of approximately 200 nm and an enhanced drug release profile with 95.20% cumulative release, indicating its potential for site-specific colon-targeted therapy. The primary objective of

this study was to develop an effective targeted nanocarrier system for 5-FU to improve its therapeutic index in colon cancer treatment. By leveraging the unique properties of MG and the cross-linking strategy, this approach offers a promising alternative to conventional 5-FU administration by reducing systemic toxicity and improving patient outcomes. Future perspectives include further optimization of the formulation to enhance the drug release efficiency, stability, and scalability. The investigation of alternative cross-linking agents or nanoparticle compositions could lead to improved therapeutic efficacy. Additionally, in-depth pharmacokinetic and pharmacodynamic studies followed by preclinical and clinical trials are essential to validate the safety and effectiveness of the formulation in human subjects. Scaling up the production and developing a commercially viable formulation could pave the way for its potential clinical application in colon cancer treatment.

## Data availability

The data used to support the findings of this study are available from the corresponding author upon request.

Received: 3 January 2025; Accepted: 21 May 2025

Published online: 26 May 2025

## References

1. Colon Targeting A novel drug delivery system. *NeuroQuantology* **20**, 549–569 (2022).
2. Valencia-Lazcano, A. A. et al. 5-Fluorouracil nano-delivery systems as a cutting-edge for cancer therapy. *Eur. J. Med. Chem* **246**, 114995 (2023).
3. Muhammed, R. A., Mohammed, S., Visht, S. & Yassen, A. O. A Review on Development of Colon Targeted Drug Delivery System. *International Journal of Applied Pharmaceutics* vol. 16 12–27 at (2024). <https://doi.org/10.22159/ijap.2024v16i2.49293>
4. Babu1, A., \*, J. S. Y. & Gupta3, D. Gupta4, A. Recent advancement in drug delivery system for brain: an overview. *World J. Pharm. Pharm. Sci.* 292–305. <https://doi.org/10.20959/wjpps20177-9454> (2017).
5. Dureja, H., Loebenberg, R., Singh, S. K., Dhanasekaran, M. & Dua, K. Advanced drug delivery systems for colonic disorders. *Adv. Drug Deliv Syst. Colon Disord.* 1–439. <https://doi.org/10.1016/C2022-0-03099-3> (2023).
6. Sopyan, I., Komarudin, A. D. P., Huang, J. A. & Insan Sunan, K. S. An overview: development of Colon drug delivery system and its application and limitations. *Int. J. Appl. Pharm.* **15**, 24–30 (2023).
7. Barathan, M. et al. Innovative strategies to combat 5-Fluorouracil resistance in colorectal cancer: the role of phytochemicals and extracellular vesicles. *Int. J. Mol. Sci.* **25**, 7470 (2024).
8. Desai, A., Mohammed, T., Patel, K. N., Almajam, M. & Kim, A. S. 5-Fluorouracil Rechallenge after cardiotoxicity. *Am. J. Case Rep.* **21**, 1–7 (2020).
9. Pourmadadi, M. et al. Innovative nanomaterials for cancer diagnosis, imaging, and therapy: drug delivery applications. *J. Drug Deliv. Sci. Technol* **82**, 104357 (2023).
10. Rahmani, M., Pourmadadi, M., Abdouss, M., Rahdar, A. & Díez-Pascual, A. M. Gelatin/polyethylene glycol/g-C<sub>3</sub>N<sub>4</sub> hydrogel with Olive oil as a sustainable and biocompatible nanovehicle for targeted delivery of 5-fluorouracil. *Ind. Crops Prod.* **208**, 117912 (2024).
11. Hossein Karami, M. & Abdouss, M. Cutting-edge tumor nanotherapy: advancements in 5-fluorouracil Drug-loaded Chitosan nanoparticles. *Inorg. Chem. Commun.* **164**, 112430 (2024).
12. Deshpande, R. D., Gowda, D. V. & Mahammed, N. Design of Pistacia lentiscus (mastic gum) controlled release spheroids and investigating the influence of roll compaction. *Ind. Crops Prod.* **44**, 603–610 (2013).
13. Speight, T. M. & Holford, N. Avery's Drug Treatment. 4th edition. *Ugeskr. Laeger* 159, 4627 (1997).
14. Yang, H. C. & Hon, M. H. The effect of the molecular weight of Chitosan nanoparticles and its application on drug delivery. *Microchem J.* **92**, 87–91 (2009).
15. Salerno, S., Ståhlberg, A., Holdfeldt, A., Bexé Lindskog, E. & Landberg, G. 5-Fluorouracil treatment of Patient-Derived scaffolds from colorectal Cancer reveal clinically critical information. *J. Transl. Med.* **20**(1), 209 (2022).
16. Yin, J. et al. Reevaluating Disease-Free survival as an endpoint vs overall survival in stage III adjuvant Colon cancer trials. *J. Natl. Cancer Inst.* **114**, 60–67 (2022).
17. Gvozdeva, Y. & Staynova, R. pH-Dependent drug delivery systems for ulcerative colitis treatment. *Pharmaceutics* **17**, 226 (2025).
18. Crispino, R. et al. Advanced polymeric systems for colon drug delivery: from experimental models to market applications. *Soft Matter.* **21**, 792–818 (2025).
19. Salaudeen, H. D. & Akinniranye, R. D. Precision nanotechnology for early Cancer detection and biomarker international journal of research publication and reviews precision nanotechnology for early Cancer detection and biomarker identification. (2024). <https://doi.org/10.55248/gengpi.5.1124.3404>
20. Sun, T. et al. Engineered nanoparticles for drug delivery in cancer therapy. *Angewandte Chemie - International Edition* vol. 53 12320–12364 at (2014). <https://doi.org/10.1002/anie.201403036>
21. Sun, T. et al. Engineered nanoparticles for drug delivery in Cancer Therapy \*. *Nanomaterials Neoplasms*. 31–142. <https://doi.org/10.1201/9780429027819-2> (2020).
22. Sharifi, M. et al. An updated review on EPR-Based solid tumor targeting nanocarriers for Cancer treatment. *Cancers (Basel)* **14**(12), 2868 (2022).
23. Khan, K. U. et al. Overview of nanoparticulate strategies for solubility enhancement of poorly soluble drugs. *Life Sci.* **291**, 120301 (2022).
24. Blanco, E., Shen, H. & Ferrari, M. Principles of nanoparticle design for overcoming biological barriers to drug delivery. *Nat. Biotechnol.* **33**, 941–951 (2015).
25. Torchilin, V. P. Recent advances with liposomes as pharmaceutical carriers. *Nat. Rev. Drug Discov.* **4**, 145–160 (2005).
26. Ferrari, M. Cancer nanotechnology: opportunities and challenges. *Nat. Rev. Cancer.* **5**, 161–171 (2005).
27. Kang, J. S., Wanibuchi, H., Salim, E. I., Kinoshita, A. & Fukushima, S. Evaluation of the toxicity of mastic gum with 13 weeks dietary administration to F344 rats. *Food Chem. Toxicol.* **45**, 494–501 (2007).
28. Sowjanya, H. & Ahad, H. Mastic gum aided amoxicillin trihydrate gastro retentive mucoadhesive microspheres: in vivo evaluation. *Bangladesh J. Sci. Ind. Res.* **57**, 187–194 (2022).
29. Bala, R., Rana, R. & Madaan, R. Formulation design and optimization of sustained released matrix tablets of propranolol Hcl using natural and synthetic polymers. *Acta Pharm. Sci.* **59**, 321–341 (2021).
30. Nasr, M. & Saad, I. E. Formulation and evaluation of mastic gum as a compression coat for colonic delivery of 5-fluorouracil. *Int. J. Drug Deliv.* **3**, 481–491 (2011).
31. Chaurasia, M. et al. Cross-linked Guar gum microspheres: A viable approach for improved delivery of anticancer drugs for the treatment of colorectal cancer. *AAPS PharmSciTech.* **7**(3), 74 (2006).
32. Liu, H. & Gao, C. Preparation and properties of ionically cross-linked Chitosan nanoparticles. *Polym. Adv. Technol.* **20**, 613–619 (2009).

33. Wu, J., Wang, Y., Yang, H., Liu, X. & Lu, Z. Preparation and biological activity studies of Resveratrol loaded ionically cross-linked chitosan-TPP nanoparticles. *Carbohydr. Polym.* **175**, 170–177 (2017).
34. Bajpai, A. K. & Likhitkar, S. Investigation of magnetically enhanced swelling behaviour of superparamagnetic starch nanoparticles. *Bull. Mater. Sci.* **36**, 15–24 (2013).
35. Gowda, D. V., Khan, M. S. & Vineela, S. Development and evaluation of phosphated Cross-Linked Guar gum microspheres for improved delivery of anticancer drug to Colon. *Polym. - Plast. Technol. Eng.* **51**, 1395–1402 (2012).
36. Ministry of environment and forests, I. SOP\_Committee for the purpose of control and supervision of experiments on animals. Compend. CPCSEA. 1–144 (2010). 1–144 (2010). (2018).
37. Laferriere, C. A. & Pang, D. S. Review of intraperitoneal injection of sodium pentobarbital as a method of euthanasia in laboratory rodents. *J. Am. Assoc. Lab. Anim. Sci.* **59**, 254–263 (2020).
38. Kilkenny, C., Browne, W. J., Cuthill, I. C., Emerson, M. & Altman, D. G. Improving bioscience research reporting: the arrive guidelines for reporting animal research. *PLoS Biol* **8**(6), e1000412 (2010).
39. Gulati, D., Arora, D., Taneja, Y. & Dhingra, A. Method development and validation of Stability-Indicating HPLC-UV method for determination of 5-Fluorouracil. *Curr Spectrosc. Chromatogr* **10**, 8 (2024).
40. Azeez, O. S. Leonardo electronic journal of practices and technologies production of gum from cashew tree latex. *Leonardo Electron. J. Pract. Technol.* **7**, 7–22 (2005).
41. Prusty, A. K. & Sahu, S. K. Biodegradable Nanoparticles - A novel approach for oral administration of biological products. *Int. J. Pharm. Sci. Nanotechnol.* **2**, 503–508 (2009).
42. Maassen, S., Fattal, E., Müller, R. H. & Couvreur, P. Cell cultures for the assessment of toxicity and uptake of polymeric particulate drug carriers. *S.T.P. Pharma Sciences* vol. 3 11–22 at (1993).
43. Sinko, P. J. & Singh, Y. *Martin's physical pharmacy and pharmaceutical sciences: physical chemical and biopharmaceutical principles in the pharmaceutical sciences: sixth edition. Martin's Phys. Pharm. Pharm. Sciences: Phys. Chem. Biopharm. Principles Pharm. Sciences: Sixth Edition* (2013).
44. Chaudhari, P. S., Slunkhe, K. S., Amrutkar, P. P., Chaudhari, S. V. & Oswal, R. J. Formulation and development of colon specific drug delivery using dextrin. *International Journal of Pharma and Bio Sciences* vol. 3 P269–P276 at (2012).
45. Halbert, G. Pharmaceutical development. *Textb Pharm. Med.* **8**, 81–100 (2009). *6th Ed.*
46. Cardot, J. M., Beyssac, E. & Alric, M. In vitro–in vivo correlation: importance of dissolution in IVIVC. *Dissolution Technol.* **14**, 15–19 (2007).

### Author contributions

Funding acquisition, Writing (UM, NM, TR, ST and AFW) Conceptualisation (Ab. A, AA, AHA, SK and UM), Investigation and methodology, (NM, TR, ST, Ab. A, and SK), Review and Supervision (UH, NM).

### Funding

The authors extend their appreciation to the Deanship of Scientific Research at King Khalid University for funding this study through Large Groups (RGP.2/78/46).

### Declarations

### Ethics approval and consent to participate

The Institutional Animal Ethical Committee at Raghavendra Institute of Pharmaceutical Education and Research-Autonomous in Andhra Pradesh approved this project (code: 878/PO/Re/S/05/CPCSEA).

### Competing interests

The authors declare no competing interests.

The in vivo procedure was performed in accordance with the guidelines of the Committee for Control and Supervision of Experiments on Animals (CCSEA). All in-vivo work is complied with the ARRIVE criteria. This study was conducted in accordance with ARRIVE guidelines.

### Conflict of interest

The authors declare no conflict of interest, financial or otherwise.

### Additional information

**Correspondence** and requests for materials should be addressed to N.M.

**Reprints and permissions information** is available at [www.nature.com/reprints](http://www.nature.com/reprints).

**Publisher's note** Springer Nature remains neutral with regard to jurisdictional claims in published maps and institutional affiliations.

**Open Access** This article is licensed under a Creative Commons Attribution-NonCommercial-NoDerivatives 4.0 International License, which permits any non-commercial use, sharing, distribution and reproduction in any medium or format, as long as you give appropriate credit to the original author(s) and the source, provide a link to the Creative Commons licence, and indicate if you modified the licensed material. You do not have permission under this licence to share adapted material derived from this article or parts of it. The images or other third party material in this article are included in the article's Creative Commons licence, unless indicated otherwise in a credit line to the material. If material is not included in the article's Creative Commons licence and your intended use is not permitted by statutory regulation or exceeds the permitted use, you will need to obtain permission directly from the copyright holder. To view a copy of this licence, visit <http://creativecommons.org/licenses/by-nc-nd/4.0/>.

© The Author(s) 2025